

Rayleigh-Instability-Induced Metal Nanoparticle Chains Encapsulated in Nanotubes Produced by Atomic Layer Deposition

Yong Qin, Seung-Mo Lee, Anlian Pan, Ulrich Gösele, and Mato Knez*

Max-Planck-Institute of Microstructure Physics, Weinberg 2, D-06120 Halle, Germany

Received August 28, 2007; Revised Manuscript Received November 23, 2007

ABSTRACT

Cu nanoparticle chains encapsulated in Al_2O_3 nanotubes were successfully generated in a controlled manner by reduction of CuO nanowires embedded in Al_2O_3 at a sufficiently high temperature. The Al_2O_3 coating was deposited by atomic layer deposition (ALD). The particles mainly show a rodlike shape and are regularly distributed. The particle diameters and chain lengths corresponding to the inner diameters and lengths of the tubes, respectively, are controlled by the size of the CuO nanowire templates. Rayleigh instability, assisted by the uniform volume shrinkage created by the reduction of oxide to metal, is proposed to induce the formation of the nanochains. This method may potentially be extended to the synthesis of nanochains of other metals by reducing corresponding oxide nanowires embedded in ALD shells.

Compared with randomly dispersed nanoparticles, assemblies of nanoparticles such as chains, rings, and three-dimensional superlattices can produce new collective physical properties, which can find applications in plasmon waveguides for photonic devices, supracrystals, chemical and biosensing applications, etc.^{1–5} Moreover, these properties are considerably affected by the particle size, shape, interparticle spacing, organized pattern, and the environment. It is therefore an important issue to precisely control the assembly of nanoparticles. Various methods based on guides from colloidal chemistry, lithography, biomolecules, and template agents are available for realization of ordered structures.^{6–11} Here, we report on the assembly of metal nanoparticles into chains encapsulated in nanotubes with well-controlled particle sizes and spacings. The organization is induced by the Rayleigh instability within a shell, which is produced by atomic layer deposition (ALD). The obtained nanochains are freestanding, which is favorable for subsequent mounting or handling.

The concept of Rayleigh instability originates from the instability of liquid cylinders due to surface tension. A liquid cylinder tends to undulate its free surface with a wavelength, which is larger than the circumference of the cylinder. The driving force for the surface undulation is the decrease of the surface area and thus the total surface energy. Plateau initiated this study over a century ago.¹² Lord Rayleigh continued with theoretical studies on the instability of liquid jets and explained the regular spacing of the formed drops.¹³ Nichols and Mullins extended Rayleigh's perturbation ap-

proach to solids.¹⁴ Recently, more effort has been put into this study in both theoretical and experimental fields leading to significant progress.^{15–18} Cu and Au nanowires on a SiO_2 substrate were observed to undergo various configurational changes to finally break up into chains of nanospheres due to Rayleigh instability with gradually increased annealing temperature.^{19,20} Also, Rayleigh instability in polymers confined within nanoporous alumina membranes was studied, which results in the formation of polymer nanorods with periodically encapsulated holes.²¹

ALD is a growth technique that utilizes the sequential exposure of the substrate to reactants to achieve monolayer-by-monolayer growth allowing an atomic-scale thickness control. As a result, growth is surface controlled instead of source controlled, enabling highly controllable deposition of conformal films on substrates with complex geometries, even porous structures.^{22–27} In this work, starting from CuO nanowires, ALD of Al_2O_3 was applied to obtain a core-shell structure. This shell effectively constrains the space of Cu during subsequent reduction of CuO in a H_2 atmosphere. The voids within the Al_2O_3 tubes, due to volume shrinkage created by the reduction of oxide to metal, provides the possibility of Rayleigh instability to occur at elevated temperatures. Our experimental results demonstrate the fabrication of well-organized nanoparticle chains confined in nanotubes by making use of both volume shrinkage and the Rayleigh instability effect.

Figure 1 schematically illustrates our synthetic approach. A three-step process was used to prepare the nanoparticle

* Corresponding author. E-mail: mknez@mpi-halle.de.

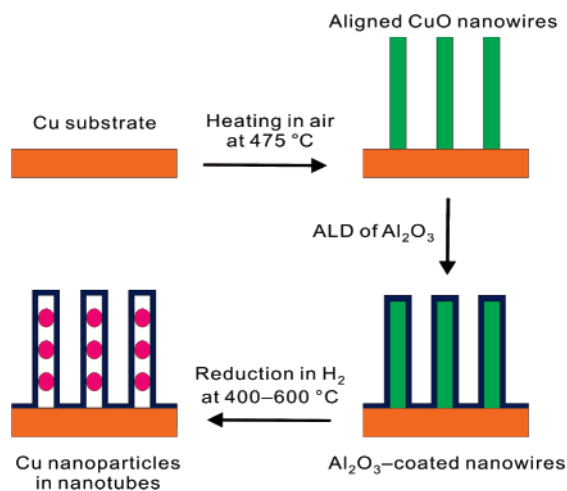


Figure 1. A schematic diagram of the preparation process of Cu nanoparticle chains confined in Al_2O_3 nanotubes.

chains encapsulated in nanotubes. At first, aligned CuO nanowires were prepared by heating Cu substrates in air.²⁸ In this work, bare transmission electron microscope (TEM) Cu grids (3.05 mm in diameter, Plano, Germany) were used as substrates for convenience and directly applied for subsequent TEM analysis after every process step. Prior to growth, the grids were cleaned by sonication in anhydrous ethanol for 10 min. Then they were transferred to an oven and heated in air at 475 °C for 2 h to obtain CuO nanowires. Subsequently, deposition of a thin Al_2O_3 layer on CuO nanowires was carried out in a commercial hot-wall flow-type ALD reactor (SUNALE R75, Picosun, Finland) at 200 °C at a pressure of 9 Torr. $\text{Al}(\text{CH}_3)_3$ and deionized H_2O were used as aluminum precursor and oxygen reactant sources, respectively, and were delivered to the reactor as ambient-temperature vapors. During the deposition process, the CuO nanowires were alternately exposed to TMA and H_2O in the ALD chamber. The pulsing time was 0.1 s for both TMA and water with N_2 as carrier gas with a flow rate of 200 sccm. A purging time of 4 s was used for both precursors. Purging was done with N_2 gas with a flow rate of 600 sccm. The thickness of the Al_2O_3 shell can be conveniently controlled by the number of pulse/purge cycles. The growth rate for Al_2O_3 was about 1.0 Å per cycle. In our study, a total number of 50 cycles were used, which gave a thickness of about 5 nm as measured from TEM images. Finally, after the ALD process, the CuO nanowires coated with Al_2O_3 were transferred to a furnace for reduction. H_2 (5% in Ar at atmospheric pressure) was used as reducing gas. The samples were heated to 400–600 °C at a rate of 50 °C/min and held for 1 h to obtain Cu nanoparticle chains. The Al_2O_3 shells are chemically stable under H_2 in this temperature range.

After the Cu grid substrates were heated in air at elevated temperatures, their color changed from red to black. From scanning electron microscopy (SEM) investigations, Cu substrate surfaces covered by well-aligned CuO nanowires could be observed (Figure S1 in Supporting Information). Figure 2a shows a TEM image of CuO nanowires after they were coated with Al_2O_3 after 50 ALD cycles. The diameters of these nanowires range from 30 to 150 nm and their lengths

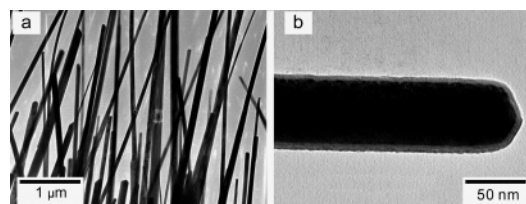


Figure 2. (a) TEM image of CuO nanowires coated with a 5 nm Al_2O_3 layer after 50 ALD cycles; (b) TEM image of an individual $\text{Al}_2\text{O}_3/\text{CuO}$ core-shell nanowire at higher magnification.

are up to 10 μm after a growth time of 2 h. From the high magnification image of an individual nanowire shown in Figure 2b, a conformal, uniform, amorphous Al_2O_3 layer of about 5 nm thickness is clearly visible with brighter contrast as compared to the CuO core. Selected area electron diffraction (SAED) pattern (Figure S2 in Supporting Information) of the CuO core can be indexed to the diffraction spots of monoclinic CuO indicative of a bicrystal structure, consistent with those previously reported.²⁸

After reduction in H_2 at 400–600 °C, the CuO nanowires coated with a 5 nm Al_2O_3 layer changed their color from black to red optically. Considering the volume shrinkage by 43% according to the density ratio of Cu to CuO, one would expect that the reduced cores are Cu nanowires with a smaller diameter as compared to that of their parent templates or coaxial Cu nanotubes closely contacting the inner wall of the Al_2O_3 shells depending on the wetting behavior of Cu. However, TEM investigations reveal that the CuO nanowires are reduced to produce nanoparticles, which show a chainlike pattern. The particles are encapsulated within the Al_2O_3 tubes, the initial shells, and are regularly separated. The particle diameters and chain lengths correspond to the inner diameters and lengths of the tubes, respectively, originally controlled by the size of the CuO nanowires. This is in strong contrast to CuO nanowires without Al_2O_3 shells, which undergo morphological changes and collapse or coalesce to form films during reduction.²⁹

Figure 3a shows the resulting samples after reduction at 400 °C. It can be observed that the starting nanowires undergo morphological changes to become dispersed nanoparticles with clear spacings except some nanowires produce longer sections. Detailed investigations at higher magnification reveal that the diameter of the nanowires has some influence on the final morphology of the nanoparticles. As displayed in Figure 3b, the nanowires with larger diameters (around 100 nm), which arise from the diameter distribution of the grown CuO nanowires, decay into long sections of several hundred nanometer length, and they have irregular morphologies with a clear surface roughness, while the nanowires with a smaller diameter (around 40 nm) fragment into almost equally spaced nanoparticles in a chainlike order. This indicates that larger diameters are not advantageous to produce perfect fragmentation into chainlike particle alignment at this temperature.

TEM images of the sample after reduction at 500 °C are displayed in Figure 3c,d. All nanowires now show nanoparticle chains. Long sections due to larger diameters of the initial CuO cores cannot be observed. From the image at

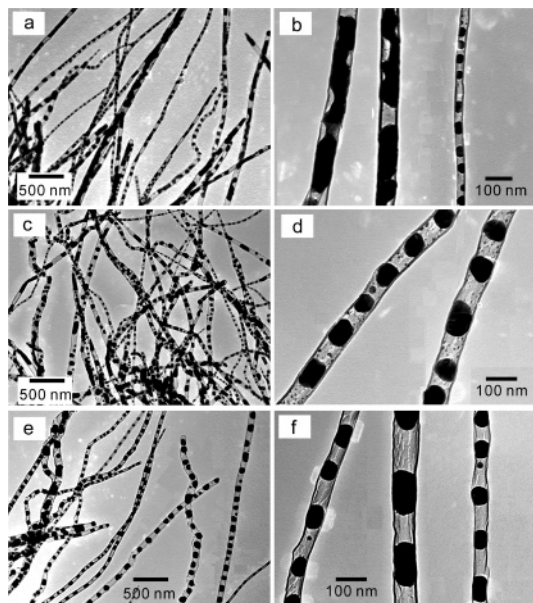


Figure 3. TEM images of Cu nanoparticle chains prepared by reduction of CuO nanowires with a 5 nm Al_2O_3 shell in H_2 for 1 h at various temperatures: (a,b) sample prepared at 400 °C; (c,d) sample prepared at 500 °C; (e,f) sample prepared at 600 °C. Panels b, d, and f are TEM images corresponding to panels a, c, and e at higher magnification. Note that the white shadows near some tubes result from defocused features due to different heights.

higher magnification (Figure 3d), it can be noted that besides the main particles there are some small particles of several nanometers in diameter, dispersed on the inner wall surface of the Al_2O_3 tubes. We assume that those small particles originate from unfinished ripening reactions.

When the reduction temperature is further increased to 600 °C, significant morphological changes in the products are observed from TEM images as shown in Figure 3e,f. The wires are perfectly fragmented into nanoparticle chains along the whole length of the tubes. The particles within one single tube have more uniform and regular shapes and their two end surfaces are more spherical than those of particles produced at 400 and 500 °C. The particles usually exhibit elongated rodlike shapes and are well distributed with relatively regular spacings. Their diameters correspond to the inner diameters of the tubes, which are determined by the starting CuO wires. Moreover, there are almost no small nanoparticles dispersed on the inner wall surfaces of the tubes. The spacings between two adjacent particles are in the same order as the length of the particles. As shown in Figure 3f, the particles have a diameter of 60–100 nm and a length of about 60–120 nm, while the spacings between two adjacent particles are about 100 nm. The SAED pattern of the nanoparticles can be indexed to the face-centered cubic structure of Cu and exhibit a single-crystalline nature (Figure S3 in Supporting Information).

The above investigations reveal that chainlike Cu nanoparticles encapsulated in nanotubes can be obtained by reduction of Al_2O_3 -coated CuO nanowires at 400–600 °C. Recently, Kim et al. investigated the reduction of CuO powders in a H_2 atmosphere by in situ time-resolved X-ray diffraction.³⁰ They found that the reduction involves an

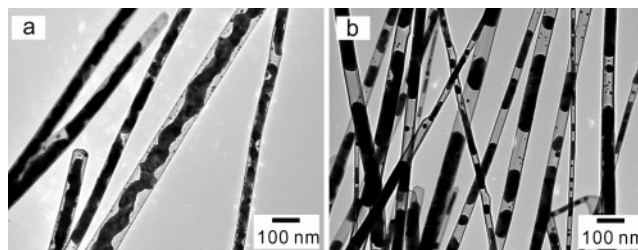


Figure 4. (a) TEM images of CuO nanowires with 5 nm Al_2O_3 shells after reduction in H_2 at 300 °C for 1 h; (b) TEM images of sample prepared by annealing the prerduced sample (at 300 °C) at 600 °C for 1 h.

induction period, which becomes shorter with increasing temperature. CuO starts to reduce after a period of 50 min, and the reduction process is completed after 200 min at 200 °C. These times are 20 and 40 min, respectively, at 250 °C. In this study, we also attempted to reduce $\text{Al}_2\text{O}_3/\text{CuO}$ nanowires at 250 and 300 °C. However, the wires were only partially reduced to produce some wires with irregular morphologies at 250 °C for 1 h (Figure S4 in Supporting Information). This is reasonable considering that the Al_2O_3 layer can hinder the diffusion of H_2 into the tubes and thus lower the reduction rate.³¹ At 300 °C, the wires can be reduced. However, they also form long sections with irregular morphologies, as shown in Figure 4a. The failure to obtain nanoparticle chains shows that a sufficiently high temperature is essential for the fragmentation of the wires. To know whether the formation of the chains completely depends on Rayleigh instability due to the high temperature, additional experiments were performed by annealing the prerduced product (at 300 °C) at 600 °C for 1 h. The experimental results reveal that only long nanorods are formed, as shown in Figure 4b. Their morphologies differ from those of the samples reduced directly at 600 °C. These results imply that not only the high temperature, but also the reduction plays an important role for the fragmentation of the wires into nanoparticle chains.

Reduction experiments of CuO nanowires with an increased number of ALD cycles of Al_2O_3 were performed to investigate the influence of the shell thickness on the product morphologies. It was found that upon increasing the thickness of Al_2O_3 an increase of the reduction temperature to obtain regular nanoparticle chains becomes necessary. Figures 5a,b show TEM images of the reduced CuO nanowires with a 20 nm Al_2O_3 shell (200 ALD cycles) at 600 °C. Although the wires decay into particles, they have no regular shapes and are not regularly spaced. Moreover, there are many small nanoparticles dispersed on the inner wall surface of the tubes (Figure 5b), similar to the CuO wires with a 5 nm Al_2O_3 shell after reduction at 500 °C (Figure 3c,d). However, when the reduction temperature was further increased to 750 °C, regularly spaced nanoparticle chains without small particles dispersed on the inner wall surface of the tubes can be successfully obtained, as shown in Figure 5c,d. The increase of the reduction temperature due to thicker shells to obtain regular nanochains further reveals that the high temperature is not the determining factor for the formation of the

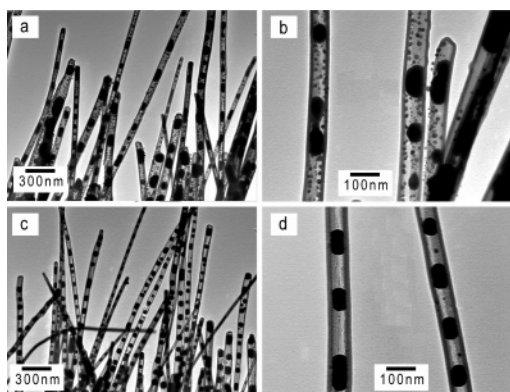


Figure 5. TEM images of Cu nanoparticle chains prepared by reduction of CuO nanowires with 20 nm Al_2O_3 shells in H_2 for 1 h at different temperatures: (a,b) sample prepared at 600 °C; (c,d) sample prepared at 750 °C. Panels b and d are TEM images corresponding to panels a and c at higher magnification.

nanochains and that the reduction reaction also significantly contributes to the formation of the nanochains.

As mentioned above, the reduction of CuO nanowires with a 5 nm Al_2O_3 shell can form nanoparticle chains at sufficiently high temperatures (400–600 °C). This corresponds to the result reported by Molarres et al.,¹⁹ which revealed the fragmentation of Cu nanowires to particles on a SiO_2 substrate due to Rayleigh instability by annealing at 400–600 °C. However, in our study we failed to produce nanochains by annealing the prereduced product (at 300 °C) at 600 °C. Moreover, the increase of thickness of the Al_2O_3 shells did not yield regular nanochains in the same temperature range; nanochains can be produced only at further increased temperatures. These results indicate that both the reduction process and the high temperature play important roles for the formation of nanochains. Therefore, it can be concluded that the uniform diffusion of the H_2 into the tubes is significant for the uniform reduction of CuO cores, which results in uniform volume shrinkage, undulation, and fragmentation under the assistance of high temperatures. At low temperatures (<400 °C), longer sections are produced (Figure 4a) relying only on volume shrinkage. Successive treatment at high temperatures fails to produce nanoparticle chains from the wires (Figure 4b). When the thickness of the shells is increased, the diffusion rate of H_2 into the shells is lowered. Possibly the diffusion dominantly depends on the defects of the shells in this case. Thus, the diffusion rate of H_2 into the shells from the defect positions would be higher. This cannot produce uniform volume shrinkage, and thus the wires fail to form well-organized nanoparticle chains (Figure 5a,b). A further increased temperature can reduce the discrepancy of the diffusion rate and again result in the formation of regularly spaced nanoparticles (Figure 5c,d). On the basis of the above scenario, a schematic is proposed to exhibit the formation mechanism for the nanochains, as shown in Figure 6. Upon heating in a H_2 atmosphere at high temperatures, the reduction of the CuO nanowires to Cu produces nanowires with a smaller diameter (Figure 6b). Then the surface diffusion of Cu atoms of the formed nanowires results in an undulation (Figure 6c). TEM investigations indeed

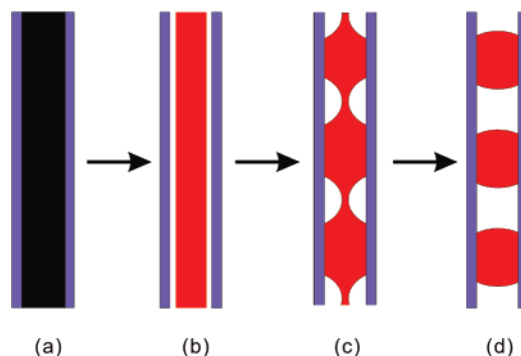


Figure 6. Formation mechanism of Cu nanoparticle chains. (a) $\text{Al}_2\text{O}_3/\text{CuO}$ core-shell nanowires; (b) reduction of the CuO core producing Cu nanowires with a smaller diameter; (c) surface diffusion of Cu atoms resulting in undulated Cu nanowires; (d) further undulation leading to final fragmentation of nanowires into nanoparticle chains.

reveal the presence of such undulated nanowires as shown in Figure 4a. Potentially those two steps (Figure 6b,c) take place simultaneously, as the results from separated reduction and fragmentation experiments (Figure 4) indicate. However, attempts to observe the intermediate state of the chain formation at higher temperatures (400–600 °C) failed in our study because of the rapid reduction reaction and fragmentation process. The process is finished within minutes of thermal treatment, thus allowing only in situ observation, which in those circumstances (temperature, H_2 gas) is instrumentally not possible with our electron microscopes. Finally, increased heating time and further undulation lead to the fragmentation of Cu nanowires into nanoparticle chains (Figure 6d).

According to the Rayleigh equation, the particle diameter D is determined by the radius R of the starting wires, namely $D = 3.78 R$, if the Cu nanowires are not confined by Al_2O_3 tubes or their radius is much thinner than that of the Al_2O_3 tubes.¹⁴ However, the radius R of the obtained Cu nanowires is too large considering the volume shrinkage ratio of 57% (the corresponding radius ratio of the obtained Cu nanowires to the initial CuO nanowires is 0.75). Therefore, this equation is not applicable here. The particle lengths and inner radii of the tubes are statistically measured for 400 particles from the chains encapsulated in 5 nm Al_2O_3 shells prepared at 600 °C. Considering the particle length as D and the inner radius of tubes as the radius of the initial CuO nanowires, the particle length D is plotted versus the radius R of the starting Cu nanowires, as shown in Figure 7. It can be seen that the particle length indeed linearly increases with the radius. However, from the slope of 2.46, indicated by the fitted line, it is obvious that the measured length indeed shows a clear discrepancy compared with the theoretical value calculated from the measured radii, as expected because of the limitations due to the spatial confinement by the Al_2O_3 nanotubes.

Ideally, the ratio of the length of the particles to the spacing should be 1.326 (57:43), based on the volume shrinkage of 43%. However, the obtained ratio is about 1.03 on average, which shows a clear deviation indicating a loss of Cu phase. This possibly results from evaporation of CuO or escaping

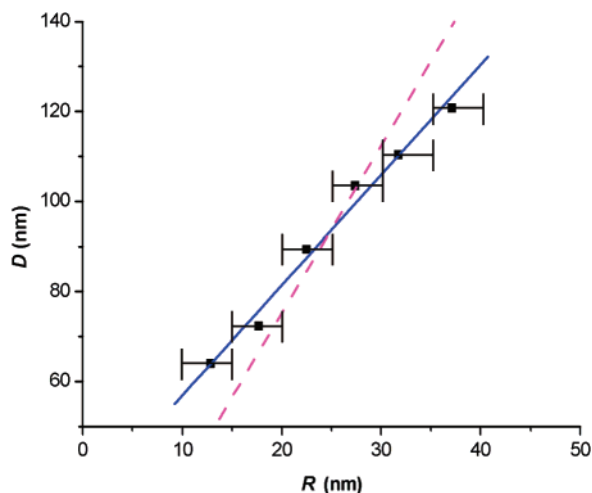


Figure 7. Plot of the particle length (D) vs the radius (R) of the starting Cu nanowires according to the average values for every 5 nm range. The solid line indicates the fitted ratio of 2.46. The dashed line indicates the theoretical ratio of 3.78.

of Cu outside of the Al_2O_3 shells at high temperatures during reduction, presumably due to defects in the shells.³² To confirm this, thermal treatment of CuO nanowires with a 5 nm Al_2O_3 shell was performed under N_2 atmosphere (900 mbar) in an oven at 600 °C for 1 h. It can be observed that there are many holes in the CuO nanowires clearly confirming that the oxide can evaporate out of the tubes, thus reducing the remaining volume (Figure S5 in Supporting Information). This also contributes partially to the discrepancy between theoretical and practical particle length.

In summary, Cu nanoparticle chains encapsulated in Al_2O_3 nanotubes can be synthesized by reduction of CuO nanowires coated with Al_2O_3 shells produced by ALD. Additionally, a coating with TiO_2 was performed leading to similar results (see Supporting Information). The chain lengths, particle lengths, and particle diameters are controlled by the size of the initial CuO nanowires. They are regularly distributed with specific interparticle distances. The formation mechanism is ascribed to Rayleigh instability together with the uniform volume shrinkage created by reduction. This method to provide space for the occurrence of Rayleigh instability by reaction can be extended to the synthesis of confined nanochains of other materials, especially of other metals by reducing corresponding oxide nanowires embedded in thin shells. The success relies on the possibility to produce highly controlled thin film coatings, for example, by ALD, and to generate space within the confinement by, for example, reducing metal oxides with a corresponding volume shrinkage. The volume ratio of metal oxide and metal should have significant impact on the possibility to produce nanoparticle chains and if they can be formed on the interparticle distance.

Acknowledgment. The authors gratefully acknowledge the financial support by the German Federal Ministry of Education and Research with the contract number FKZ: 03X5507.

Supporting Information Available: SEM image of CuO nanowires. SAED analysis of $\text{Al}_2\text{O}_3/\text{CuO}$ core-shell nanowires and copper nanoparticle chains. TEM images of CuO nanowires after reduction in H_2 at 250 °C and after thermal treating at 600 °C under N_2 atmosphere. Preparation and characterization of Cu nanoparticle chains encapsulated in TiO_2 nanotubes. This material is available free of charge via the Internet at <http://pubs.acs.org>.

References

- (1) Krenn, J. R. *Nat. Mater.* **2003**, 2, 210.
- (2) Maier, S. A.; Kik, P. G.; Atwater, H. A.; Meltzer, S.; Harel, E.; Koel, B. E.; Requicha, A. A. G. *Nat. Mater.* **2003**, 2, 229.
- (3) Redl, F. X.; Cho, K. S.; Murray, C. B.; O'Brien, S. *Nature* **2003**, 423, 968.
- (4) DeVries, G. A.; Brunnbauer, M.; Hu, Y.; Jackson, A. M.; Long, B.; Neltner, B. T.; Uzun, O.; Wunsch, B. H.; Stellacci, F. *Science* **2007**, 315, 358.
- (5) Collier, C. P.; Vossmeier, T.; Heath, J. R. *Annu. Rev. Phys. Chem.* **1998**, 49, 371.
- (6) Tang, Z. Y.; Kotov, N. A. *Adv. Mater.* **2005**, 17, 951.
- (7) Lee, S. W.; Mao, C.; Flynn, C. E.; Belcher, A. M. *Science* **2002**, 296, 892.
- (8) Mao, C.; Solis, D. J.; Reiss, B. D.; Kottmann, S. T.; Sweeney, R. Y.; Hayhurst, A.; Georgiou, G.; Iverson, B.; Belcher, A. M. *Science* **2004**, 303, 213.
- (9) Lin, Y.; Boeker, A.; He, J.; Sill, K.; Xiang, H.; Abetz, C.; Li, X.; Wang, J.; Emrick, T.; Long, S.; Wang, Q.; Balazs, A.; Russell, T. P. *Nature* **2005**, 434, 55.
- (10) Storhoff, J. J.; Mirkin, C. A. *Chem. Rev.* **1999**, 99, 1849.
- (11) Shenhar, R.; Rotello, V. M. *Acc. Chem. Res.* **2003**, 36, 549.
- (12) Plateau, J. *Transl. Annual Reports of the Smithsonian Institution*, **1873**, p. 1863.
- (13) Rayleigh, L. *Proc. London Math. Soc.* **1878**, 10, 4.
- (14) Nichols, F. A.; Mullins, W. W. *Trans. Metall. Soc. AIME* **1965**, 233, 1840.
- (15) De Gennes, P. G.; Brochard-Wyart, F.; Quere, D. *Capillarity and Wetting Phenomena*; Springer: New York, 2004.
- (16) Lian, J.; Wang, L.; Sun, X.; Yu, Q.; Ewing, R. C. *Nano Lett.* **2006**, 6, 1047.
- (17) Park, J.; Suh, K. Y.; Seo, S.; Lee, H. H. *J. Chem. Phys.* **2006**, 124, Art. No. 214710.
- (18) Kolb, F. M.; Hofmeister, H.; Zacharias, M.; Gösele, U. *Appl. Phys. A* **2005**, 80, 1405–1408.
- (19) Toimil-Molaes, M. E.; Balogh, A. G.; Cornelius, T. W.; Neumann, R.; Trautmann, C. *Appl. Phys. Lett.* **2004**, 85, 5337.
- (20) Karim, S.; Toimil-Molaes, M. E.; Balogh, A. G.; Ensinger, W.; Cornelius, T. W.; Khan, E. U.; Neumann, R. *Nanotechnology* **2006**, 17, 5954.
- (21) Chen, J. T.; Zhang, M. F.; Russell, T. P. *Nano Lett.* **2007**, 7, 183.
- (22) George, S. M.; Ott, A. W.; Klaus, J. W. *J. Phys. Chem.* **1996**, 100, 13121.
- (23) Ritala, M.; Leskela, M. In *Handbook of Thin Film Materials*; Nalwa, H. S., ed.; Academic: San Diego, CA, 2002; Volume 1, p 103.
- (24) Puurunen, R. L. *J. Appl. Phys.* **2005**, 97, 121301.
- (25) Knez, M.; Kadri, A.; Wege, C.; Gösele, U.; Jeske, H.; Nielsch, K. *Nano Lett.* **2006**, 6, 1172.
- (26) Fan, H. J.; Knez, M.; Scholz, R.; Nielsch, K.; Pippel, E.; Hesse, D.; Zacharias, M.; Gösele, U. *Nat. Mater.* **2006**, 5, 627.
- (27) Knez, M.; Nielsch, K.; Niinistö, L. *Adv. Mater.* **2007**, 19, 3425.
- (28) Jiang, X. C.; Herricks, T.; Xia, Y. *Nano Lett.* **2002**, 2, 1333.
- (29) Qin, Y.; Staedler, T.; Jiang, X. *Nanotechnology* **2007**, 18, 035608.
- (30) Kim, J. Y.; Rodriguez, J. A.; Hanson, J. C.; Frenkel, A. I.; Lee, P. L. *J. Am. Chem. Soc.* **2003**, 125, 10684.
- (31) Groner, M. D.; Fabreguette, F. H.; Elam, J. W.; George, S. M. *Chem. Mater.* **2004**, 16, 639.
- (32) Guo, Y. F.; Guo, W. L. *Nanotechnology* **2006**, 17, 4726.

NL0721766